JB Journals.ASM.org

Involvement of PG2212 Zinc Finger Protein in the Regulation of Oxidative Stress Resistance in *Porphyromonas gingivalis* W83

Yuetan Dou,[a] Wilson Aruni,[a] Tianlong Luo,[b] Francis Roy,[a] Charles Wang,[a,c] Hansel M. Fletcher[a,d]

Division of Microbiology and Molecular Genetics, School of Medicine, Loma Linda University, Loma Linda, California, USA[a]; School of Life Sciences, Fudan University, Shanghai, China[b]; Center of Genomics, School of Medicine, Loma Linda University, Loma Linda, California, USA[c]; Institute of Oral Biology, Kyung Hee University, Seoul, Republic of Korea[d]

The adaptation of *Porphyromonas gingivalis* to H_2O_2-induced stress while inducible is modulated by an unknown OxyR-independent mechanism. Previously, we reported that the PG_2212 gene was highly upregulated in *P. gingivalis* under conditions of prolonged oxidative stress. Because this gene may have regulatory properties, its function in response to H_2O_2 was further characterized. PG2212, annotated as a hypothetical protein of unknown function, is a 10.3-kDa protein with a cysteine 2-histidine 2 (Cys_2His_2) zinc finger domain. The isogenic mutant *P. gingivalis* FLL366 (ΔPG_2212) showed increased sensitivity to H_2O_2 and decreased gingipain activity compared to the parent strain. Transcriptome analysis of *P. gingivalis* FLL366 revealed that approximately 11% of the genome displayed altered expression (130 downregulated genes and 120 upregulated genes) in response to prolonged H_2O_2-induced stress. The majority of the modulated genes were hypothetical or of unknown function, although some are known to participate in oxidative stress resistance. The promoter region of several of the most highly modulated genes contained conserved motifs. In electrophoretic mobility shift assays, the purified rPG2212 protein did not bind its own promoter region but bound a similar region in several of the genes modulated in the PG_2212-deficient mutant. A metabolome analysis revealed that PG2212 can regulate a number of genes coding for proteins involved in metabolic pathways critical for its survival under the conditions of oxidative stress. Collectively, our data suggest that PG2212 is a transcriptional regulator that plays an important role in oxidative stress resistance and virulence regulation in *P. gingivalis*.

Porphyromonas gingivalis, a black-pigmented Gram-negative anaerobic bacterium, has been recognized as a major pathogen in adult periodontitis and is associated with other inflammatory systemic diseases, including cardiovascular disease and rheumatoid arthritis (reviewed in references 1 and 2). To facilitate adaptation to the oxidative changes in the periodontal pocket, survival of the organism within this dynamic inflammatory microenvironment would require a protective mechanism(s) which can rapidly be modulated. This attribute, especially among anaerobic bacteria, is a vital component that can determine their virulence and pathogenic potential.

Several systems, including antioxidant enzymes (reviewed in reference 3), DNA binding proteins (4), the hemin layer (5, 6), and enzymatic removal of deleterious products, for example 8-oxoG, caused by reactive oxygen species (ROS) (7), can defend and protect *P. gingivalis* against oxidative stress-induced damage. The expression of antioxidant-related genes is usually regulated by transcriptional modulators that sense oxidative-stress-generating agents. For example, when exposed to oxidative stresses, *Escherichia coli* induces one or both of two regulatory systems, the OxyR and SoxRS regulons (8). Expression of OxyR-regulated genes (OxyR regulons) is induced by the transcription factor OxyR, activated by peroxides such as hydrogen peroxide (8). Several transcriptional regulators associated with oxidative stress, including extracytoplasmic function (ECF) sigma factors, have been identified in *P. gingivalis* (9); however, homologs for *soxR* or *soxS* have not been identified in this organism (10). Further, in contrast to *E. coli* or *Bacteroides fragilis*, *oxyR* in *P. gingivalis* is not inducible under hydrogen peroxide-induced oxidative stress and appears to play a role in aerotolerance in the organism (11, 12). While other studies have shown that the RprY response regulator may be associated with oxidative stress resistance in *P. gingivalis*, its mechanism is still unclear (13). Taken together, there is a gap in our understanding of the OxyR-independent inducible oxidative stress resistance mechanism(s) in *P. gingivalis*.

Previously, we have assessed the transcriptome response of *P. gingivalis* to conditions of oxidative challenge depending on the duration or level of exposure (6). This study indicated that *P. gingivalis* has an adaptive response to oxidative stress that may involve several previously unrecognized genes. Moreover, bacterial cells exposed to a shorter duration of H_2O_2 revealed increased expression of genes involved in DNA repair, while after a longer duration, genes involved in protein fate, protein folding, and stabilization were upregulated (6). The gene encoding PG2212, annotated as a hypothetical protein, was found to be induced after a prolonged exposure to H_2O_2 (6). Bioinformatics analysis revealed that this protein is a putative transcriptional regulator and contains a cysteine 2-histidine 2 (Cys_2His_2) zinc finger DNA-binding motif. In this report, we have further characterized PG2212. As a transcriptional regulator with DNA promoter binding properties, we have demonstrated its ability to play an important role in the regulation of oxidative stress resistance and virulence in *P. gingivalis*.

Received 2 June 2014 **Accepted** 2 September 2014

Published ahead of print 15 September 2014

Address correspondence to Hansel M. Fletcher, hfletcher@llu.edu.

Supplemental material for this article may be found at http://dx.doi.org/10.1128/JB.01907-14.

Copyright © 2014, American Society for Microbiology. All Rights Reserved.

doi:10.1128/JB.01907-14

TABLE 1 Strains and plasmids used in this study

Strain or plasmid	Relevant characteristic(s)	Reference or source
Strains		
W83	Wild type	Dou et al. (9)
FLL366	ΔPG_2212::*ermF*	This study
FLL366 C	FLL366 with pFLL366a	This study
FLL388	*E. coli* BL21 with pET0594	This study
FLL390	*E. coli* BL21 with pFN2212	This study
Plasmids		
pVA2198	Sp^r, *ermF-ermAM*	Fletcher et al. (24)
pT-COW	Ap^r, *tetQ*	Gardner et al. (26)
pFLL366a	Ap^r, *tetQ*, Tc::PG_2212	This study
pET102-TOPO	Ap^r, His tag	Life Science Inc.
pFN2A	Ap^r, GST	Promega Inc.
pET0594	Ap^r, PG_0594	This study
pFN2212	Ap^r, PG_2212	This study

MATERIALS AND METHODS

Bioinformatic analysis. The DNA and amino acid sequences were aligned using Bioedit (http://www.mbio.ncsu.edu/bioedit/bioedit.html) and were analyzed using MEGA version 4.0 (14). The amino acid sequences were analyzed using ClustalW version 2.0 (http://www.ebi.ac.uk/). The signal peptide and potential cleavage sites were predicted using both Neural network and hidden Markov model (15). The localization studies, conserved domain architecture, and transmembrane prediction were determined using the NCBI software and hidden Markov models (16).The secondary structure prediction and modeling of the protein were performed using the Modeler software package (17). The models were validated using the WHAT IF program (18). Metabolic pathway analysis was carried out using the Kyoto Encyclopedia of Genes and Genomes (KEGG) (www.genome.jp/kegg/) (19), based on the information from the online databases Biosilico (20), BRENDA (21), and ExPASy Enzyme (22).

Bacterial strains, plasmids, and culture conditions. Strains and plasmids used in this study are listed in Table 1. *P. gingivalis* strains were cultured as described previously (9). In brief, *P. gingivalis* in brain heart infusion (BHI) broth was supplemented with yeast extract (0.5%), hemin (5 μg/ml), vitamin K (0.5 μg/ml), and DL-cysteine (0.1%). *P. gingivalis* strains were grown in an anaerobic chamber in 10% H_2, 10% CO_2, and 80% N_2 at 37°C. Growth rates for *P. gingivalis* strains were determined spectrophotometrically by measuring the optical density at 600 nm (OD_{600}). The concentration of erythromycin used was 10 μg/ml, and that of tetracycline was 0.3 μg/ml.

Sensitivity to hydrogen peroxide. Sensitivity of *P. gingivalis* strain to hydrogen peroxide was tested as previously reported (23). In brief, hydrogen peroxide at a final concentration of 0.25 mM was added to the early-log-phase cultures (OD_{600}, ~0.2), and these were further incubated at 37°C for 27 h. The OD_{600} was measured at 3-hour intervals over the 27-hour period. Cell cultures without hydrogen peroxide were used as controls.

Construction of the PG_2212 deficiency mutant. Long PCR-based fusion of several fragments was done as previously described (9). Primers used in this study are listed in Table 2. One-kilobase flanking fragments both upstream and downstream of PG_2212 were PCR amplified from chromosomal DNA of *P. gingivalis* W83. The promoterless *ermF* cassette was amplified from the plasmid pVA2198 (24) by using oligonucleotide primers that contained 24 or 25 overlapping nucleotides for the upstream and downstream fragments. These three fragments were then fused together by PCR using the forward primer, PG2212_F1, of the upstream fragment and the reverse primer, PG2212_R3, of the downstream fragment. The fusion PCR program consisted of 1 cycle of 5 min at 94°C, followed by 30 cycles of 30 s at 94°C, 30 s at 54°C, and 3 min 30 s at 68°C, with a final extension of 5 min at 68°C. The purified fused fragment was used to transform *P. gingivalis* W83 by electroporation as previously described (25). The cells were plated on BHI agar containing 10 μg/ml of erythromycin and incubated at 37°C for 7 days. The correct gene replacement in the erythromycin-resistant mutants was confirmed by colony PCR and DNA sequencing.

Complementation of the PG_2212-deficient mutant (FLL366). A DNA fragment containing the PG_2212 open reading frame (ORF) was amplified from chromosomal DNA of *P. gingivalis* W83 using primer sets PG2212_Com_F and PG2212_Com_R (Table 2). The *ragA* promoter was amplified by using primer set Rag-A-P_F and Rag-A-P_R as listed in Table 2. A BamHI restriction site was designed at the 5′ end of both primers Rag-A-P_F and PG2212_Com_R to facilitate the subcloning of the PCR fragment. The PG_2212 ORF was fused to the *ragA* promoter by PCR using the Rag-A-P_F and PG2212_Com_R primers (Table 2). Both the BamHI-digested pT-COW (26) and the PCR fragment were ligated together and used to transform *E. coli* DH5α. The purified recombined plasmid, designated pFLL366a, was used to transform *P. gingivalis* FLL366 (ΔPG_2212::*ermF*) by electroporation.

Gingipain activity assays. The activity of Rgp and Kgp protease was determined by using a method previously reported (27). In brief, arginine gingipain activity was measured with 1 mM BAPNA (*N*α-benzoyl-DL-arginine-*p*-nitroanilide) as the substrate in an activated protease buffer (0.2 M Tris-HCl, 0.1 M NaCl, 5 mM $CaCl_2$, 10 mM L-cysteine, pH 7.6). Lysine gingipain activity was measured with ALNA (Ac-Lys-p-nitroanilide HCl) as the substrate. After incubation of the substrate and culture, the reaction was stopped by the addition of 50 μl of glacial acetic acid. The OD_{405} was then measured against a blank sample containing no protease.

DNA microarray. DNA microarray was carried out using Roche NimbleGen custom arrays (100910_CW_P_ging_W83_expr_HX12) according to the standard NimbleGen procedure (NimbleGen arrays user's guide, Gene Expression Analysis v5.1). Briefly, total RNA was extracted from *P. gingivalis* using the SV Total RNA isolation kit (Promega), and cDNA was synthesized by using the High Fidelity cDNA synthesis kit (Roche). The quality of both RNA and cDNA was checked using Agilent Bioanalyzer and Agilent RNA 6000 nano and DNA 1000 chips. cDNA (0.5 to 1 μg) was used in the amplification and labeling reaction using the NimbleGen one-color labeling kit, in which Cy3/Cy5 was randomly incorporated in the newly synthesized DNA with Klenow fragment. Two micrograms of labeled cDNA derived from each RNA sample was hybridized with each array for over 16 to 18 h. All experiments were done in triplicates. The slides/arrays were washed and spun dry and then scanned using the Roche Microarray MS200 scanner with a resolution of 2 μm. The normalization was done using the NimbleScan 2.6.0.0 built-in normalization function. Microarray data analysis was performed using Partek Genomics Suite (v6.5). Differentially expressed genes were determined using a fold change of ≥1.5 and *P* values of ≤0.05, with a false-discovery rate (FDR) of 0.05.

qPCRs. The primers of differentially expressed genes are listed in Table 2. Amplification was performed with the SYBR green kit (Qiagen), and real-time fluorescence signal was detected by using the Cepheid Smart Cycler Real Time PCR apparatus. Real-time quantitative PCRs (qPCRs) were performed as follows: 95°C for 15 min, followed by 40 cycles of 94°C for 15 s, 54°C for 30 s, and 72°C for 30 s. Each measurement was performed in triplicate for each gene. 16S rRNA genes were used as an internal control to normalize variations due to differences in reverse transcription efficiency.

PG_2212 target promoter motif prediction. The promoter regions of genes up- or downregulated were analyzed by using the online SCOPE software. Briefly, 200-bp lengths of DNA sequence upstream of start codon ATG or TTG containing putative promoter were aligned using SCOPE (http://genie.dartmouth.edu/scope/).

Overexpression and purification of rPG0594. The PG_0594 ORF was amplified by PCR and then ligated to the expression vector pET102/D-TOPO (Invitrogen, Inc.). The primers used are listed in Table 2. The

TABLE 2 Primers used in this study

Use and name of primer	Sequence (5′–3′)
Mutant construction	
PG2212_F1	CTTTCGTACATCGTCGATTGGGACA
PG2212_R1	TCATTTATTCCTCCTAGTTAGTCACTCAATACCGAACGCCCGTCGGCTA
PG2212_F3	TTCGTAGTACCTGGAGGGAATAATCATCTGAACGGACAGTTTGCCATGTA
PG2212_R3	CTACGGTACTCCTCGGATTGCGGCT
Erm_F_f(5)	TGACTAACTAGGAGGAATAAATGACAAAAAAGAAATTGCCCG
Erm_F_r(3)	GATTATTCCCTCCAGGTACTACGAAGGATGAAATTTTTCA
Complementation of PG2212 deficiency mutant	
Rag-A-P_F	TCGGATCCTTGCAGAAATTTCTGCATTTGTGGT[a]
Rag-A-P-R	GGATCTGTATAGGACTTCTCTCAAAGACTTTTCTTTTGCGTTAAACTT
PG2212-com-F	TTGAGAGAAGTCCTATACAGATCCGACA
PG2212-com-R	TGGATCCTCAGATTGTTTGCGTTCGGAA[a]
Overexpression of PG0594 and PG2212	
PG0594-ET-F	CACCATGAGGCAACTTAAAATTTCCAA[b]
PG0594-ET-R	GCCGAGATAACCTTTCAGATTCTT
PG2212-Ex_F	GGCGATCGCCATGAGAGAAGTCCTATACAGAT[c]
PG2212-Ex_R	CGTTTAAACTCAGATTGTTTGCGTTCGGAAAA[d]
EMSA	
PG2212_EMSA_F	GTCTCACAAGAGGCCTCCCA
PG2212_EMSA_R	GGATAAACCTCTACATTAACCGTTGA
PG1167_EMSA_F	GGCAAAATAATGGCAAGGAAGTCAT
PG1167_EMSA_R	GAACGAAAGGGTCGTTTCGGTA
PG1459_EMSA_F	CGGTAATGCGAGGAGGAGTTATTT
PG1459_EMSA_R	CTTCGGGTAAAGTGTCAAGGCCT
PG1167_EMSA_Fs	CCGCTTTTCAATGGAATAAACCGC
PG1167_EMSA_Rs	CCTTGGAAAAACGGAAAAAGATGGC
PG1459_EMSA_Fs	CGTCTAAAGCTCGGAGTGTGC
PG1459_EMSA_Rs	AGCCCACGAAACGAAATCGGCA
Real-time qPCR	
16S_Realtime_F	CGAGAGCCTGAACCAGCCAAGT
16S_Realtime_R	GATAACGCTCGCATCCTCCGTATTA
PG2212_realtime_F	GATATCCGGGGCTCTCCTCTTCT
PG2212_realtime_R	CAGAACGAAAAAAATCTCGCGCCACTT
PG0521_Realtime_F	CATTGGCAGACCGCGTACTTGTA
PG0521_Realtime_R	GCTTTGAGCACCATCTCTTCGTCT
PG1775_Realtime_F	CGCAGCCGAAGAGAACGACAA
PG1775_Realtime_R	CACGAGCACCTTTTCTCCTCCAT
PG1208_Realtime_F	CGATACCGCTCTCGACAAACTGA
PG1208_Realtime_R	GACCTTGAGCACCGCCGAAGT
PG0138_Realtime_F	CGTCACCGATCCGGCAGAGA
PG0138_Realtime_R	CCGTTGTCGCTTCAGGAGCAATT
PG1167_Realtime_F	GGATCGGAGAAAAGCAGAGCATG
PG1167_Realtime_R	CCCTTATTTAGAATCATTCCAAACTCGT
PG0985_Realtime_F	CGAGGAGGCTGAGGATGCCA
PG0985_Realtime_R	GCCTTTCGGATCAGGTTCAGGCA
PG1237_realtime_F	CACCGGCTACAAGATACAATTCATA
PG1237_realtime_R	TCCCGATACGAGTGGATTCATGA
PG0708_realtime_F	GCTTCTCGTACAATCTGGGAGC
PG0708_realtime_R	GCTTCATGGCGATAGATACGGT
PG0709_realtime_F	GTTTGTTGTATCGTGTCTTGAAGGA
PG0709_realtime_R	GCATCAGACAAACACCCTCAGT
PG2117_realtime_F	GGTGTTAAGAAGGGTGCTTTCGAT
PG2117_realtime_R	GCTACAGCGGCTTCTTTCACCTT
PG1178_realtime_F	TCGTGGCCATTCTTCTCTTCCA
PG1178_realtime_R	CAGCTCACCTCTCACTCTCGTA
PG0352_realtime_F	CCAGGATTATCGTACAGGGAGA
PG0352_realtime_R	CCGATATATAAGTGCGCTGAGGA
vimA_realtime_F	CATACATTTGACTTCGAAGGTTCCA

(Continued on following page)

TABLE 2 (Continued)

Use and name of primer	Sequence (5′–3′)
vimA_realtime_R	GGCTCGCCATTTACGTCTTAGT
PG1237_realtime_F	CACCGGCTACAAGATACAATTCATA
PG1019_realtime_F	CACCCGGATCAGTACTTCGTCATA
PG1019_realtime_R	GGTATAGATCATGGAAAGGACGATG
PG1181_realtime_F	CGAAGAGACGACAAAGGAGTTCA
PG1181_realtime_R	ATCCTTGAAGTGCTCCAACGACGA
PG1171_realtime_F	TGCACGATGACCTGAAGATCACCA
PG1171_realtime_R	CCTTGTTGTGGTACGGTCGGT
PG1421_realtime_F	CAGTTGTGTAGCATGCGGATCAT
PG1421_realtime_R	GGCAGGATGGATAGCTTCAGAA
5′-RACE	
5′RACE Outer primer	GCTGATGGCGATGAATGAACACTG
PG2212_EMSA_R	GGATAAACCTCTACATTAACCGTTGA

[a] Underlining indicates the BamHI restriction site.
[b] Underlining indicates the pET102 vector overhang.
[c] Underlining indicates the SgfI restriction site.
[d] Underlining indicates the PmeI restriction site.

forward primer with an extra 5′-CACC-3′ at the 5′ end and the stop codon was removed in the reverse primer in order to produce a protein containing a His_6 tag. The recombined plasmid was then transformed into *E. coli* BL21(DE3) (Invitrogen, Inc.). Overexpression of pET102-0594 was induced by 1 mM IPTG (isopropyl-β-D-thiogalactopyranoside) at 16°C. The recombinant PG0594 protein (rPG0594) containing a His_6 tag at the C terminus was purified from *E. coli* BL21 cell lysate by using nickel-nitrilotriacetic acid (Ni-NTA) beads (Qiagen) according to the manufacturer's guidelines. In brief, rPG0594-containing cell lysate was incubated with magnetic beads coated with Ni-NTA in binding/washing buffer (50 mM Na-phosphate [pH 8.0], 300 mM NaCl, 0.01% Tween 20) for 30 min at room temperature and then washed four times with binding/washing

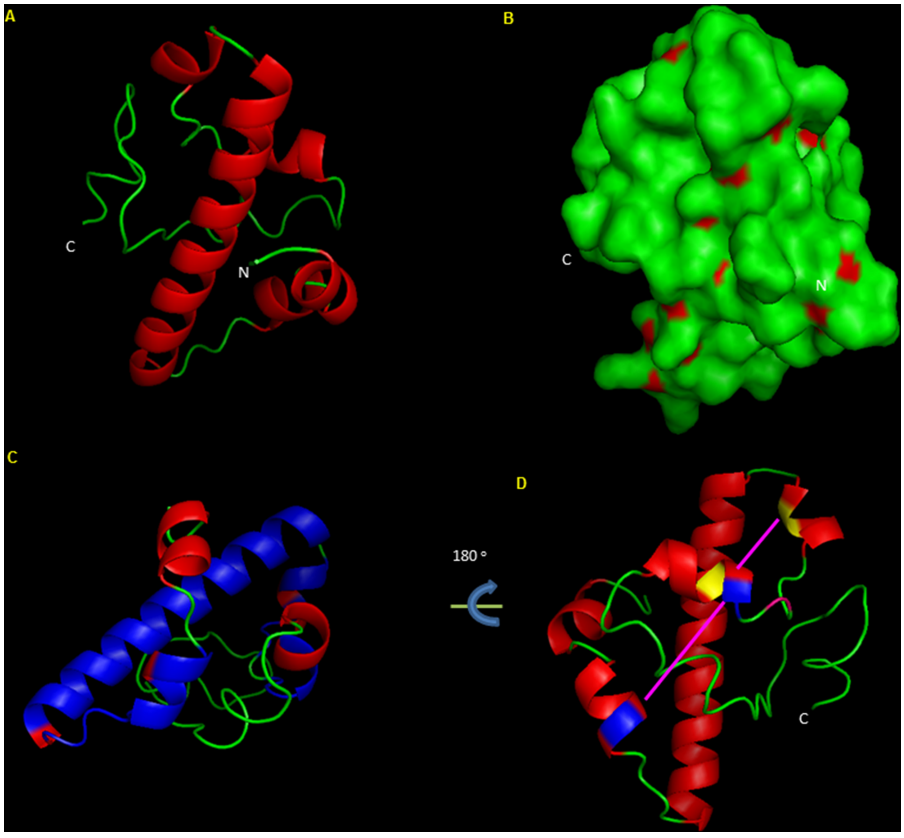

FIG 1 *In silico* protein modeling and analysis of PG2212, a protein of 94 amino acids in length, showing the Cys_2His_2 zinc finger domain. (A) Model of PG2212, showing protein structure containing a helix and loop structure devoid of beta sheets. (B) Model of PG2212 showing hydrophobic residues (red) on the surface of the protein. (C) Model of PG2212 showing the C-terminal zinc finger domain coupled with domain DUF1661 (blue). (D) Model of PG2212 showing the DNA-binding zinc finger motif with histidine residue (blue) and cysteine residue (yellow). C, C terminus; N, N terminus.

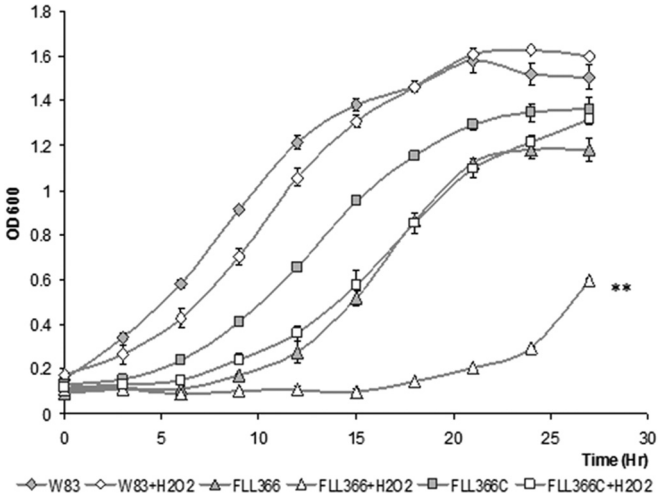

FIG 2 The PG_2212-deficient mutant showed more sensitivity to 0.25 mM hydrogen peroxide than did the wild type. Strains grown to the early log phase were treated with 0.25 mM H_2O_2 and further incubated for 27 h. The cultures without H_2O_2 were used as controls. All values are means ± standard errors from three independent experiments (**, $P < 0.001$).

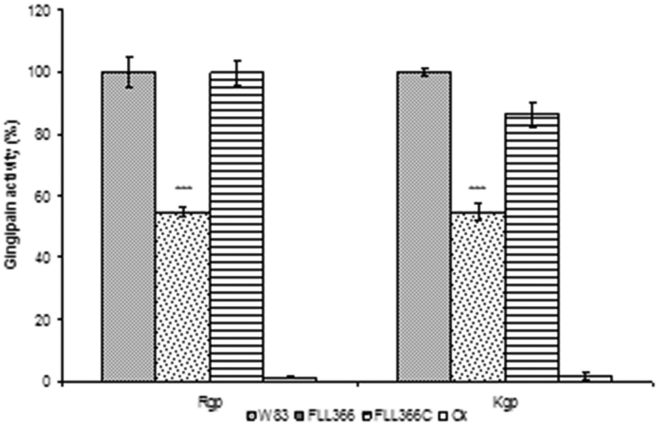

FIG 3 Gingipain activity in *P. gingivalis* FLL366. *P. gingivalis* strains were grown to the stationary phase in BHI medium supplemented with hemin and vitamin K. Activities against Rgp or Kgp were tested in whole-cell cultures. The gingipain activities were normalized to that of W83 (set as 100%), and the mutants' activities were reported as a percentage thereof. The results shown were representative of at least three independent replicates, and asterisks indicate results significantly different from those of W83 ($P < 0.005$).

buffer. Proteins binding to the NTA beads were eluted by using elution buffer (300 mM imidazole, 50 mM Na-phosphate [pH 8.0], 300 mM NaCl, 0.01% Tween 20). Eluates were then analyzed by SDS-PAGE and immunoblot analysis.

Overexpression and purification of rPG2212. The PG_2212 ORF was amplified by PCR using primers as listed in Table 2. The forward primer was engineered with an SgfI (AsiI) restriction site, while the reverse primer carried a PmeI restriction site 5′-GTTTAAAC-3′. The PG_2212 PCR product was digested by SgfI and PmeI and then ligated to SgfI- and PmeI-digested expression vector pFN2A (Promega, Inc.). The recombined plasmid, designated pFN2212, was then transformed into the *E. coli* strain BL21(DE3) (Invitrogen, Inc.). Overexpression of pFN2212 was induced by 1 mM IPTG at 16°C. The recombinant PG2212 protein (rPG2212) fused with glutathione *S*-transferase (GST) protein at the N terminus was purified from cell wall/cell membrane-free cell lysates of *E. coli* BL21 (28), refolded by dialysis using buffers containing series concentrations of urea (29), and further purified using MagneGST beads (Promega) according to the manufacturer's guidelines. In brief, rPG2212-GST-containing cell lysate was incubated with magnetic beads in binding/washing buffer (4.2 mM Na_2HPO_4, 2 mM K_2HPO_4, 140 mM NaCl, 10 mM KCl) for 30 min at room temperature and then washed four times with binding/washing buffer. Proteins binding to the MagneGST beads were eluted by using elution buffer (50 mM glutathione [pH 7.0 to 8.0]–50 mM Tris-HCl [pH 8.1]). Eluates were then analyzed by SDS-PAGE and immunoblot analysis.

Immunoblot analysis. SDS-PAGE was performed as reported previously (30). The separated proteins were then transferred to Bio-Trace nitrocellulose membranes (Pall Corporation, Ann Arbor, MI) and processed at 15 V for 25 min with a SemiDry Trans-blot apparatus (Bio-Rad). The blots were probed with primary antibodies against the His tag (mouse) or GST protein (rabbit) (Invitrogen, Inc.), and the secondary goat anti-mouse or goat anti-rabbit antibodies were horseradish peroxidase conjugated (Zymed Laboratories). Immunoreactive proteins were detected by the procedure described in the Western Lightning Chemiluminescence Reagent Plus kit (Perkin-Elmer Life Sciences, Boston, MA).

EMSA. The promoter regions of the genes of interest were PCR amplified using primers listed in Table 2. The PCR fragments were then labeled with biotin using the Biotin 3′ end DNA labeling kit (Thermo Scientific). The electrophoretic mobility shift assay (EMSA) was performed according to the manufacturer's guidelines (Thermo Scientific). In brief, 1 μg of purified rPG0594 or rPG2212 was mixed with 10 fmol of biotin-DNA and binding buffer (10 mM Tris, 50 mM KCl, 1 mM dithiothreitol [DTT], pH 7.5) and incubated at room temperature for 30 min. The samples were resolved in 5% polyacrylamide nondenaturing gel and analyzed by using a chemiluminescence kit (Thermo Scientific).

5′ RLM-RACE assay. For 5′ RNA ligase-mediated rapid amplification of cDNA ends (5′ RLM-RACE) assay, total RNA was isolated using the SV Total RNA Isolation kit (Promega) from the wild-type W83 culture grown to an OD_{600} of 0.8 to 1.0. The transcription start site was determined by 5′-RACE using the First Choice RLM-RACE kit (Ambion). The forward primer used for nested PCR was the 5′ RACE Outer primer from the kit, and the reverse primer used was PG2212_EMSA_R as listed in Table 2. The PCR fragments were ligated into the pCR2.1-TOPO vector (Invitrogen), which was then used to transform the *E. coli* Top10 competent cells. The inserts in the recombinant plasmid were confirmed by PCR, and DNA sequencing was done using the M13 reverse primer (Eton Bioscience, Inc.).

RESULTS

PG2212 is upregulated under oxidative stress. Prolonged exposure to oxidative stress in *P. gingivalis* induced a 2.7-fold increase expression in the PG_2212 gene (6). To further confirm its induction under oxidative stress conditions, *P. gingivalis* was exposed to 0.25 mM H_2O_2 for 15 min and the expression of the PG_2212 gene was evaluated by quantitative real-time PCR. In contrast to cells grown under normal anaerobic conditions, there was a 2.41 (± 0.43)-fold upregulation of the PG_2212 gene in those cells exposed to oxidative stress.

PG_2212 encodes a putative zinc finger protein. PG_2212 is 285 nucleotides in length and is predicated to encode a 94-amino-acid hypothetical protein of unknown function (www.oralgen.org/). With the absence of a signal peptide, localization studies predict that PG2212 is a cytoplasmic protein (see Fig. S1 in the supplemental material). Protein modeling shows a basic helix-loop-helix structural motif (Fig. 1A). The surface structure of the protein shows exposed hydrophobic residues suggestive of lipid-associated membrane contact (Fig. 1B). The domain architecture of the protein showed a cysteine 2-histidine 2 (Cys_2His_2) zinc finger motif and a DUF1661 motif of unknown function (Fig. 1C and D). A

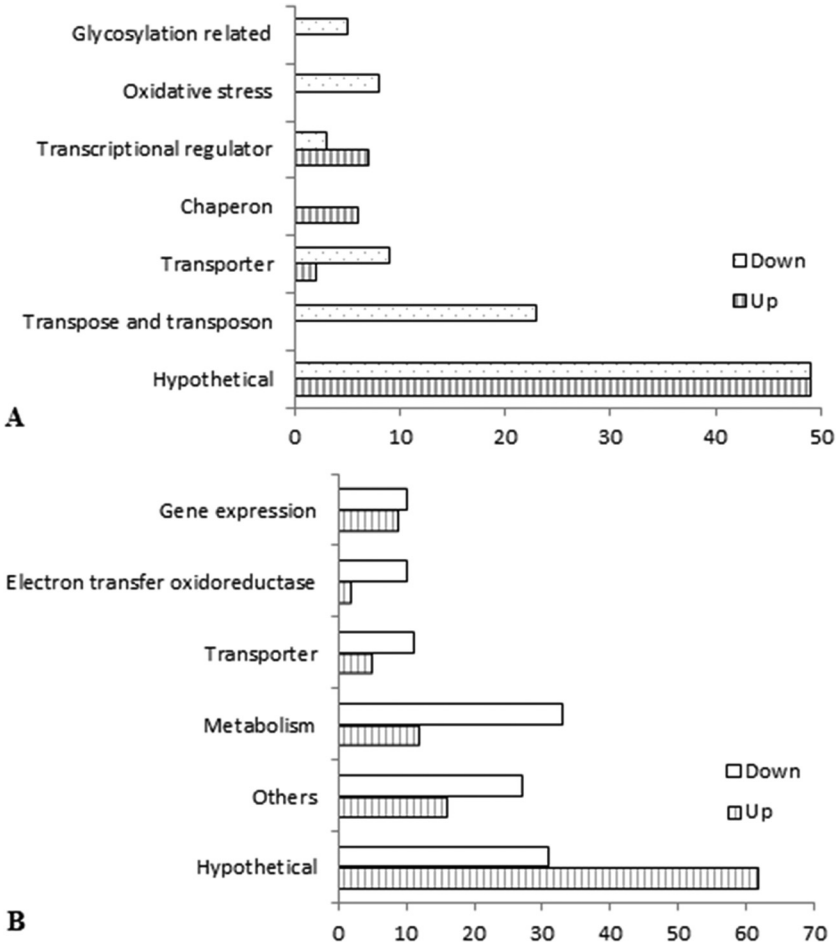

FIG 4 Distribution of functions for *P. gingivalis* FLL366 genes affected by growth under normal conditions (A) or exposure to H_2O_2 for 15 min (B). The genes that were differentially expressed ($\geq$1.5-fold up- or downregulation; $P \leq 0.05$) were grouped by functional class according to the Los Alamos *P. gingivalis* genome database (www.oralgen.org/).

sequence comparison of several of the *P. gingivalis* zinc finger domain-containing proteins showed the similar characteristic Cys-His motif (see Fig. S2 in the supplemental material). Based on the modeling of PG2212 protein, the cysteine residues at positions 33 and 44 and histidine at positions 35 and 79 along with phenylalanine at positions 32 38, 39, and 76 could bring about hydrophobic interactions and coordinate DNA binding (Fig. 1D). The DUF1661 domain is conserved among 7 different *P. gingivalis* annotated hypothetical proteins (PG2212, PG2064, PG1980, PG1904, PG1722, PG1661, and PG0524). Multiple-sequence alignment of these proteins also showed zinc finger motifs suggesting possible DNA binding properties (see Fig. S3 in the supplemental material). Taken together, since zinc finger proteins are reported to be part of a large family of nucleic acid binding proteins and could function as transcriptional regulators, it is likely that PG2212 may have a regulatory role in response to oxidative stress.

The PG2212-deficient mutant showed increased sensitivity to H_2O_2-induced oxidative stress. To further confirm a functional role for PG_2212 in oxidative stress protection, an isogenic mutant of *P. gingivalis* deficient in this gene was constructed by allelic-exchange mutagenesis. The PG2212-deficient mutants were selected on BHI agar plates carrying erythromycin. Deletion of the PG_2212 gene in the erythromycin-resistant isogenic mutants was confirmed by colony PCR and DNA sequencing (data not shown). To compare their phenotypic properties with those of wild-type strain W83, all erythromycin-resistant colonies were plated onto BHI blood agar plates. Similar to the wild-type strain, they all displayed a black-pigmented phenotype. One mutant, designated *P. gingivalis* FLL366, was randomly chosen for further study. Although there was a longer lag phase for *P. gingivalis* FLL366 in broth culture than for the parent strain, the growth rates during exponential phase appeared to be similar for both strains (Fig. 2). The PG2212-deficient mutant showed increased sensitivity to 0.25 mM hydrogen peroxide compared to the wild type (Fig. 2). Gingipain activity was reduced by more than 40% in the PG2212-deficient mutant (Fig. 3). *P. gingivalis* FLL366 complemented with the wild-type PG_2212 gene (FLL366C) restored the wild-type phenotype (Fig. 2 and 3). Taken together, these results suggest that the PG_2212 gene may play a role in tolerance to H_2O_2-induced oxidative stress and gingipain activity.

PG_2212-modulated transcriptome response of *P. gingivalis* to oxidative stress. While several OxyR-independent genes are induced in *P. gingivalis* in response to H_2O_2 (6), a mechanism for their regulation is still unclear. To investigate the effects of PG_2212 on the modulation of genes known to be involved in

TABLE 3 Genes differentially expressed in FLL366 under both anaerobic and hydrogen peroxide stress conditions

Gene ID	Annotation	HPS[a]		AN[b]	
		Fold change	*P* value	Fold change	*P* value
Downregulated					
PG_0061	YngK protein	−1.61	0.000426	−1.53	6.7E−17
PG_0195	Rubrerythrin	−2.01	0.002247	−1.66	0.00278
PG_0548	Pyruvate ferredoxin/flavodoxin oxidoreductase family protein	−2.77	0.000341	−1.64	1.5E−09
PG_0682	ABC transporter, permease protein, putative	−1.50	0.019527	−1.67	1.4E−17
PG_0683	ABC transporter, permease protein, putative	−1.75	0.001568	−1.74	1.1E−13
PG_1006	Hypothetical protein PG1006	−1.50	0.006456	−1.75	1.5E−22
PG_1172	Iron-sulfur cluster binding protein, putative	−3.41	0.000149	−1.59	7.2E−08
PG_1173	YkgG family protein	−1.96	0.000406	−1.52	7E−08
PG_1214	Hypothetical protein PG1214	−2.14	0.00121	−1.64	1.8E−22
PG_1392	Rod shape-determining protein RodA, putative	−1.62	0.001405	−1.63	5.5E−14
PG_1393	Penicillin-binding protein 2, putative	−1.59	0.000734	−1.83	3.8E−17
PG_1402	Rhomboid family protein	−1.53	0.003675	−1.63	2.9E−11
PG_1734	Transporter, putative	−1.62	0.003835	−1.66	3.1E−11
PG_1738	Hypothetical protein PG1738	−1.85	0.006191	−1.55	8.7E−13
PG_1778	Hypothetical protein PG1778	−1.51	0.016187	1.55	4.1E−13
PG_1812	2-Ketoisovalerate ferredoxin reductase	−1.20	4.66E−05	−1.57	0.03345
Upregulated under AN but downregulated under HPS conditions					
PG_0689	NAD-dependent 4-hydroxybutyrate dehydrogenase	−1.74	0.00621	1.55	1.8E−08
PG_0691	NifU-related protein	−1.52	0.011859	1.50	6E−07
Upregulated					
PG_0329	Formiminotransferase-cyclodeaminase-related protein	1.51	0.195903	1.81	4.4E−12
PG_0330	Histone-like family DNA-binding protein	1.50	0.08439	1.72	4.5E−10
PG_0495	Hypothetical protein PG0495	5.57	1.4E−05	2.38	0.00565
PG_0592	50S ribosomal protein L31 type B	1.76	0.014037	1.83	3.3E−16
PG_0612	Hypothetical protein PG0612	2.01	7.83E−05	1.50	3.2E−13
PG_0686	Hypothetical protein PG0686	2.66	0.000614	1.68	1.2E−12
PG_0707	TonB-dependent receptor, putative	2.69	7.8E−05	2.56	5.6E−17
PG_0985	ECF subfamily RNA polymerase sigma factor	3.68	0.000346	1.99	2.8E−16
PG_0986	Hypothetical protein PG0986	4.84	1.61E−05	1.89	5.8E−16
PG_0987	Hypothetical protein PG0987	5.40	1.51E−05	1.83	8.5E−15
PG_1019	Putative lipoprotein	14.88	4.43E−06	2.75	0.02315
PG_1108	Hypothetical protein PG1108	1.61	0.004065	2.13	1E−07
PG_1178	Hypothetical protein PG1178	9.23	1.62E−05	2.82	0.04231
PG_1179	Hypothetical protein PG1179	11.44	4.76E−05	2.53	0.04907
PG_1180	Hypothetical protein PG1180	11.06	1.53E−05	1.86	0.00836
PG_1181	Tetr family transcriptional regulator	4.73	9.09E−05	1.52	0.00481
PG_1236	Hypothetical protein PG1236	4.09	1.43E−06	2.81	2.5E−06
PG_1237	LuxR family transcriptional regulator	4.54	1.08E−05	3.42	3.3E−06
PG_1240	TetR family transcriptional regulator	2.62	0.000192	1.67	7.6E−12
PG_1268	Hypothetical protein PG1268	3.77	0.000276	2.40	7.8E−14
PG_1315	Peptidyl-prolyl *cis-trans* isomerase SlyD, FKBP-type	1.65	0.007939	2.04	4.5E−11
PG_1316	Hypothetical protein PG1316	1.52	0.025092	1.84	9.1E−11
PG_1497	Histone-like family DNA-binding protein	1.65	0.069685	2.12	1.1E−09
PG_1551	HmuY protein	4.82	0.000105	2.04	0.00261
PG_1552	TonB-dependent receptor HmuR	4.26	0.000935	2.17	0.00173
PG_1553	CobN/magnesium chelatase family protein	4.41	3.18E−05	2.25	0.02276
PG_1625	Hypothetical protein PG1625	4.72	2.63E−06	1.78	1.8E−08
PG_1659	Hypothetical protein PG1659	1.76	0.009558	1.89	3.2E−20
PG_1755	Fructose-1,6-bisphosphate aldolase	1.75	0.000758	1.80	1E−10
PG_1798	Immunoreactive 46-kDa antigen PG99	3.07	0.000153	1.61	3.1E−06
PG_1856	Cytidine/deoxycytidylate deaminase family protein	3.22	0.000332	1.83	0.00143
PG_1857	Hypothetical protein PG1857	5.19	0.000125	1.69	0.00514
PG_1858	Flavodoxin FldA	4.26	1.95E−05	2.65	0.10882

[a] HPS, hydrogen peroxide stress.
[b] AN, anaerobic conditions.

TABLE 4 Real-time qPCR validation of microarray analysis for selected genes differentially expressed in FLL366/W83 under anaerobic conditions

Gene ID	Annotation	Real-time qPCR		DNA microarray	
		Fold change	SD	Fold change	*P* value
PG_0138	Malonyl-CoA–acyl carrier protein transacylase	−2.93	0.093	−2.31	1.25E−07
PG_1167	Hypothetical protein PG1167	−19.11	0.004	−7.78	4.99E−08
PG_0521	Cochaperonin GroES	3.13	0.672	3.28	5.17E−13
PG_0708	Peptidyl-prolyl *cis-trans* isomerase, FKBP-type	2.26	0.244	3.11	1.29E−17
PG_0709	Peptidyl-prolyl *cis-trans* isomerase FkpA, FKBP-type	4.28	0.73	3.14	9.85E−18
PG_0985	ECF subfamily RNA polymerase sigma factor	2.38	0.342	1.99	2.83E−16
PG_1178	Hypothetical protein PG1178	19.00	4.611	2.82	0.0423073
PG_1208	Molecular chaperone DnaK	6.14	1.17	2.63	7.85E−14
PG_1237	LuxR family transcriptional regulator	3.08	0.631	3.42	3.26E−06
PG_1775	GrpE protein	1.82	0.16	2.78	5.69E−09

oxidative stress resistance in *P. gingivalis*, we performed whole-genome profiling by DNA microarray analysis. *P. gingivalis* FLL366 (ΔPG_2212::*ermF*) cells, in the exponential growth phase, were exposed to H_2O_2 for 15 min. The microarray-determined differentially expressed genes (DEGs) were classified into functional groups according to their annotation in the Oral Pathogen Sequence Databases at the Los Alamos National Laboratory (www.oralgen.org/). The results graphically presented in Fig. 4A revealed that about 11.8% (262 genes) of the *P. gingivalis* genome displayed altered expression in the PG_2212-deficient mutant under normal anaerobic conditions (fold change $\geq$ 1.5, $P \leq 0.05$, FDR $\leq$ 0.05). More genes were downregulated (130) than upregulated (120) in *P. gingivalis* FLL366 than in the wild type in response to H_2O_2 exposure at 15 min (Fig. 4B). The majority of the modulated genes were hypothetical/unassigned/unknown function (Fig. 4; see also Tables S1 and S2 in the supplemental material).

In cells grown under normal anaerobic conditions and not exposed to H_2O_2, 262 genes (including 137 genes that were upregulated and 125 genes that were downregulated more than 1.5-fold) were differentially expressed in FLL366 compared to the wild type. A comparative analysis (Table 3) showed that 16 genes were downregulated more than 1.5-fold in FLL366 by comparison to the wild-type under both anaerobic and H_2O_2 stress conditions; 2 genes were upregulated more than 1.5-fold under normal anaerobic conditions but downregulated more than 1.5-fold under H_2O_2 stress conditions; 33 genes were upregulated more than 1.5-fold under both normal anaerobic and H_2O_2 stress conditions. The pattern of expression of selected genes using real-time qPCR confirmed those observed in the DNA microarray analysis (Tables 4 and 5).

TSS mapping of the PG_2212 gene. RLM-RACE was performed to determine the start site for the transcriptional unit. As shown in Fig. 5A, a 169-bp-length DNA fragment was PCR amplified, and an adenine residue was identified as the transcription start site (TSS) by sequencing. A TTG codon annotated as the translation start codon (Fig. 5B) was observed 169 nucleotide bases downstream from the TTS. Sequences predicted to represent the −35, −10, and ribosomal binding sites were also observed upstream of the translational start codon (Fig. 5B).

rPG2212 does not bind to the PG_2212 promoter. To test whether PG2212 could be autoregulated by binding to its own promoter region, we expressed and purified the recombinant PG2212 as a glutathione (GST) fusion protein (Fig. 6A). As a control for the experiments, we also expressed and purified the sigma factor 70 protein as a His_6 fusion protein (Fig. 6B). EMSA was performed with the upstream region of PG_2212 using a PCR-amplified 200-bp DNA fragment upstream of the start of transcription. Figure 6C shows that promoter-containing DNA fragments from PG_2212 were not shifted in the presence of rPG2212. This is in contrast to the complete shift in the presence of PG0594, the sigma factor 70 protein. The PG0594 shift was inhibited by the addition of a 200-fold excess amount of unlabeled target DNA (Fig. 6D).

Modulated genes in the PG_2212-deficient mutant contain a conserved motif. The promoter regions of several of the genes most highly up- and downregulated were analyzed to determine if there were conserved regions indicative of a potential regulator site. As shown in Fig. 7, conserved motifs that have the potential to form a hairpin structure were observed to have 5′-TTTTT-3′ at positions −50 to −70 nucleotides (nt) and 5′-AAAAA-3′ at positions −103 to −125 nt. It is noteworthy that the genes upregulated

TABLE 5 Real-time qPCR validation of microarray analysis for selected genes differentially expressed in FLL366/W83 under hydrogen peroxide stress conditions

Gene ID	Annotation	Real-time qPCR		DNA microarray	
		Fold change	SD	Fold change	*P* value
PG_1171	Oxidoreductase, putative	−2.19	0.612	−3.57	0.00074138
PG_1421	Ferredoxin, 4Fe-4S	−6.58	1.505	−3.40	0.00010054
PG_1545	Superoxide dismutase, Fe-Mn	−1.78	0.389	−1.94	0.0132979
PG_0985	ECF subfamily RNA polymerase sigma factor	7.32	0.286	3.68	0.00034552
PG_1019	Putative lipoprotein	22.16	8.454	14.88	4.43E−06
PG_1181	TetR family transcriptional regulator	10.18	0.572	4.73	9.09E−05
PG_1237	LuxR family transcriptional regulator	5.37	1.689	4.54	1.08E−05

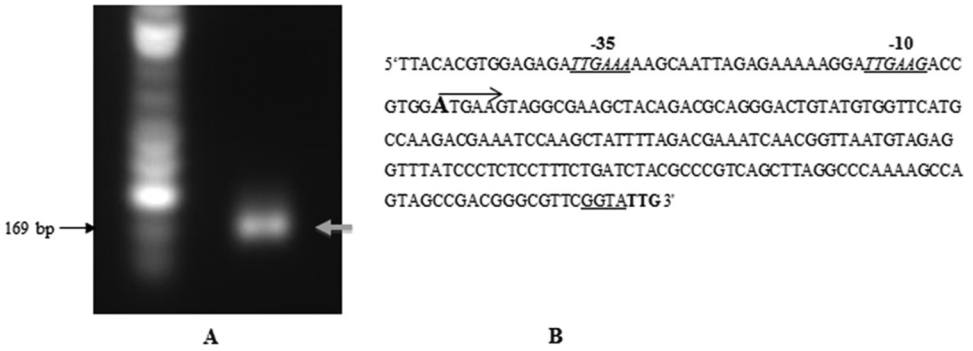

FIG 5 Identification of the transcription start site of the PG_2212 gene of *P. gingivalis* by RLM-RACE. (A) PCR amplification of the PG_2212 promoter region. (B) Promoter region of PG_2212. The transcription start site adenine is marked in bold, and the arrow indicates the direction of transcription of PG_2212; the translation start codon (TTG) is indicated in bold; the −35 and −10 motifs are italicized and underlined, and the ribosome binding sites are underlined.

in the PG_2212-deficient mutant were missing or had more variation in the consensus sequences observed from −103 to −125 nt. Additionally, a conserved motif with 5′-TCAXG-3′ sequences was observed at −40 nt.

PG_1167 and PG_1459 promoter region can bind rPG2212. Since PG_1167 and PG_1459 were the most highly downregulated genes in *P. gingivalis* FLL366 (ΔPG_2212::*ermF*) compared to the wild type (see Table S1 in the supplemental material), their promoter regions were evaluated to determine their ability to interact with the rPG2212 protein. In EMSAs, the 250-bp-length DNA fragments containing the promoter region of both genes were significantly retarded in the presence of the rPG2212 protein (Fig. 8). Additionally, the shift was inhibited by the addition of a 200-fold excess amount of the unlabeled target DNA (Fig. 8). Online analyses using software Scope (http://genie.dartmouth.edu/scope) revealed that there is a 5′-AATGGAA-3′ motif and a reversible complemented 5′-TTCCGTT-3′ motif upstream of the putative −35 motif in the promoter region of PG_1167. A similar 5′-CTCGGAG-3′ motif and reversible complemented 5′-TTTCGTT-3′ motif were found upstream of the putative −35 motif in the promoter region of PG_1459 (Fig. 9A). To further study the conserved sequence that PG2212 could bind to, the primers PG1167_EMSA_Fs, PG1167_EMSA_Rs, PG1459_EMSA_Fs, and PG1459_EMSA_Rs were designed to amplify 46-bp and 38-bp fragments containing these motifs of PG_1167 and PG_1459, respectively (Table 2), and the PCR products were designated PG1167 Fs and PG1459 Fs for PG_1167 and PG_1459, respectively. The purified rPG2212 was used in EMSA, and the results showed that rPG2212 could bind to these two DNA fragments,

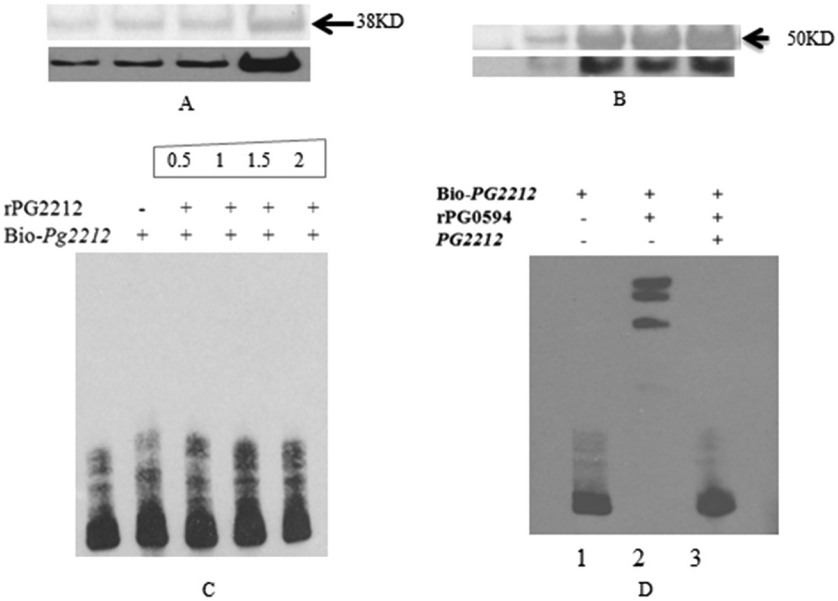

FIG 6 Electrophoretic mobility shift assay (EMSA) showed that rPG0594 could bind to the promoter of PG_2212. (A) The purified rPG2212 was analyzed by SDS-PAGE and confirmed by using anti-GST antibody. (B) The purified rPG0594 was analyzed by SDS-PAGE and confirmed by using anti-His antibody. (C) Electrophoretic mobility shift assay showed that rPG2212 could not bind to the promoter of PG_2212. The number shows the quantity (pmol) of rPG2212 protein added in the reaction system. (D) EMSA was performed using biotin-labeled DNA (0.06 pmol), protein (1 pmol), and the nonlabeled competitor DNA (6 pmol). Results showed rPG0594 binding to the promoter of PG_2212. Lane 1, biotin-labeled PG_2212; lane 2, biotin-labeled PG_2212 and rPG0594; lane 3, biotin-labeled PG_2212, rPG0594, and competitive PG_2212 promoter.

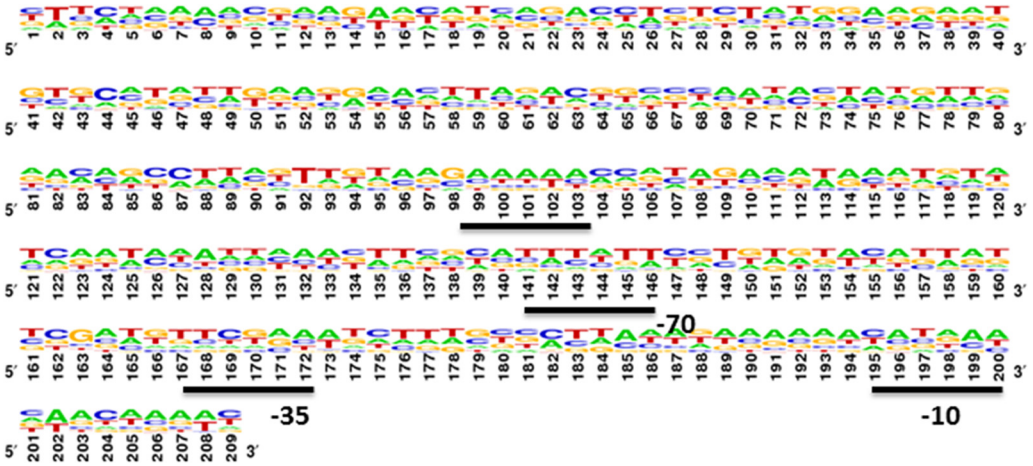

FIG 7 Promoter region analysis of all the downregulated genes shown in Table 3 and in Table S1 in the supplemental material showed three different motifs in the promoter region of genes regulated by PG2212. Poly "T" was discovered in the −70 region, and poly "A" was discovered in the −120 region.

although the retardation signal for PG_1167 was not as strong as that for PG_1459 (Fig. 9B).

PG2212 can regulate important metabolic pathways critical for survival under oxidative stress conditions. The metabolic activity of *P. gingivalis* under conditions of oxidative stress is modified to facilitate the organism to utilize alternate energy substrates and to generate by-products that may help restore a permissive environment (6). Because several genes modulated in the PG_2212-deficient mutant belonged to different biochemical pathways and contained a putative PG2212 binding motif in their promoter region, the microarray data were used to analyze the metabolome of *P. gingivalis* FLL366 during oxidative stress. As shown in Fig. 10, PG2212 regulates acetyl coenzyme A (acetyl-CoA) synthesis, leading to the modulation of many important biochemical pathways. The metabolites pyruvate, formate, butyrate, and acetate were downregulated. In contrast, the succinyl-CoA metabolite leading to fumarate was upregulated.

DISCUSSION

Adaptability to the changing environment of the periodontal pocket is critical to the survival and pathogenesis of *P. gingivalis* (reviewed in reference 31). Earlier reports have documented an inducible protective system in response to oxidative stress (3, 6). A transcriptome examination revealed that *P. gingivalis* is able to prioritize the response by first protecting and repairing its genetic material and then subsequently repairing any damaged proteins (6). A comprehensive mechanism and the transcriptional regulator(s) involved in this protective process are still unclear. In this study, we have examined the functional role of PG2212 in regulating the response of *P. gingivalis* to oxidative stress and its virulence potential.

Our study has confirmed that the inducible PG_2212 gene, which encodes a hypothetical protein, gets upregulated in *P. gingivalis* under conditions of oxidative stress. In addition to H_2O_2-induced oxidative stress, PG_2212 can also be upregulated in response to oxygen-induced oxidative stress (12) suggesting a role for this gene in a broad response to oxidative stress possibly mediated by multiple mechanisms. This is in contrast to *oxyR* in *P. gingivalis*, which is modulated only under microaerophilic conditions (11). In other bacteria, OxyR acts as a sensor for H_2O_2 and other peroxides by its reaction through a unique Cys residue (reviewed in reference 32). This oxidation changes the conformation of the tetrameric OxyR, which triggers the activation of OxyR site-specific binding to DNA promoters (33). Taken together, our observations suggest that *P. gingivalis* may use an alternate mech-

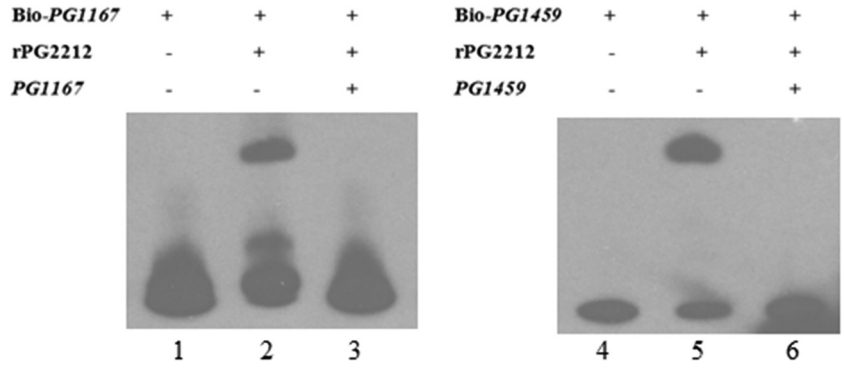

FIG 8 Electrophoretic mobility shift assay showed that rPG2212 could bind to the promoters of PG_1167 and PG_1459. Lane 1, biotin (Bio)-labeled PG_1167; lane 2, biotin-labeled PG_1167 and rPG2212; lane 3, biotin-labeled PG_1167, rPG2212, and competitive PG_1167 promoter; lane 4, biotin-labeled PG_1459; lane 5, biotin-labeled PG_1459 and rPG2212; lane 6, biotin-labeled PG_1459, rPG2212, and competitive PG_1459 promoter.

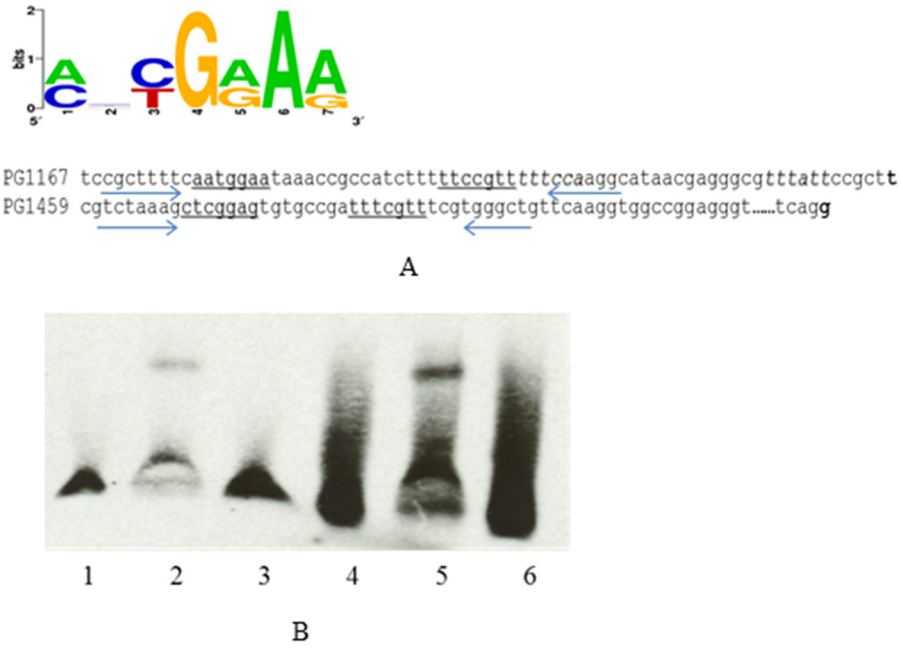

FIG 9 Electrophoretic mobility shift assay showed that rPG2212 could bind to the promoter of PG_1167 and PG_1459. (A) Promoter region of PG_1167 and PG_1459; the consensus motifs are underlined. Arrows show the primer sequence. (B) EMSA results: lane 1, biotin-labeled PG_1167 Fs; lane 2, biotin-labeled PG_1167 Fs and rPG2212; lane 3, biotin-labeled PG_1167 Fs, rPG2212, and competitive PG_1167 Fs; lane 4, biotin-labeled PG_1459 Fs; lane 5, biotin-labeled PG_1459 Fs and rPG2212; lane 6, biotin-labeled PG_1459, rPG2212, and competitive PG_1459 Fs.

anism for its direct response to H_2O_2. The response of the PG_2212 gene to oxidative stress suggests that it may play a role as part of this mechanism. This is further supported by the fact that inactivation of the PG_2212 gene in *P. gingivalis* triggered increased sensitivity to H_2O_2.

Bacteria sense and respond to redox changes primarily through sensitive thiols and metals in the sensor/regulator (reviewed in references 32, 34, and 35). Our *in silico* structural analysis of PG2212 has identified a Cys_2-His_2 zinc finger domain. Zinc fingers, first reported and widely studied in eukaryotes, can mediate

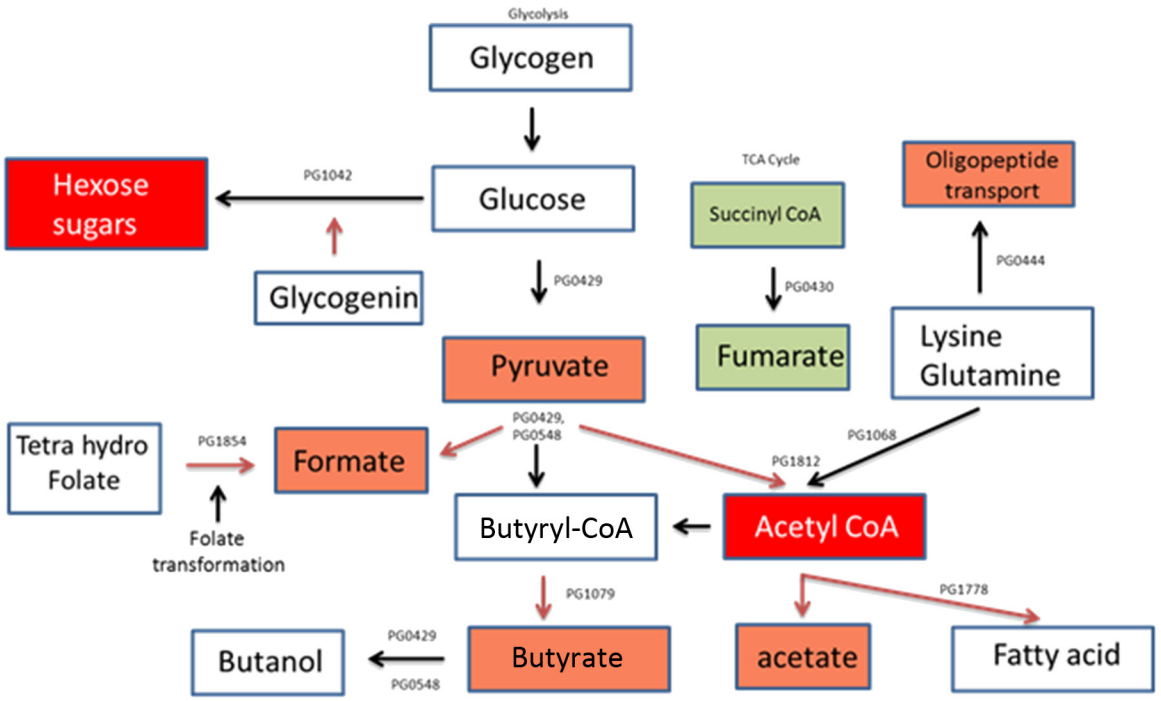

FIG 10 Metabolome analysis revealed that PG2212 is involved in regulation of acetyl-CoA synthesis and modulates other metabolic pathways. Red boxes, downregulated metabolites; green boxes, upregulated metabolites.

protein-protein, protein-RNA, and protein-ligand interactions (reviewed in reference 36). Additionally, they are a common structural element utilized by sequence-specific DNA-binding proteins to interact with DNA (37, 38). As transcription factors, these zinc finger proteins have been reported in organisms ranging from humans to bacteria. We have demonstrated that PG2212 is involved in the regulation of virulence and oxidative stress resistance of *P. gingivalis*. Its ability to bind to the promoter regions of two genes (PG_1167 and PG_1459) most highly downregulated in the PG_2212-deficient isogenic mutant suggests that it is likely a transcriptional regulator. This could be functional, similar to what occurs with Ros, the first prokaryotic Cys_2-His_2-type zinc finger transcription-regulatory protein discovered in *Agrobacterium tumefaciens* (39). Mutations in *ros* led to the upregulation of virulence genes *virC* and *virD* and also to increased expression of *ipt*, which encodes an isopentenyl transferase required for the biosynthesis of cytokinin in the host plant (39). Other similar transcriptional regulators have been described in *Enterobacteriaceae* (40, 41), *Rhizobium leguminosarum* bv. *trifolii rosR* (42), *Sinorhizobium meliloti* (43), *Rhizobium etli* (44), and *Agrobacterium radiobacter* (45).

Several regulon-carrying multiple hypothetical genes of unknown function were modulated in the *P. gingivalis* PG_2212-deficient mutant. Several genes encoding proteins predicted to be the oxidoreductase family and iron-sulfur clusters were downregulated. Collectively, these proteins may represent multiple mechanisms to scavenge the reactive oxygen species (ROS), repair damaged macromolecules, and maintain a survival metabolic state. These proteins may also be involved in sensing the oxidative stress environment and amplifying and/or coordinating the response. The iron-sulfur cluster proteins may sense and activate gene transcription. This is observed in other bacteria; for example, the Fe-S cluster-containing transcription factor IscR senses both the Fe-S cluster biosynthesis status and H_2O_2 and modulates regulation of iron and ROS metabolism, which is critical to the synergistic toxicity of these compounds (46–48). When the 2Fe-2S cluster is intact, IscR represses the transcription of genes involved in Fe-S cluster biosynthesis (49). H_2O_2 derepresses IscR gene expression by disassembling the IscR 2Fe-2S cluster and activates an alternate Fe-S assembly pathway, which is more robust toward oxidative stress (47). It is unclear if a similar mechanism is functional in *P. gingivalis*, and this is under further investigation.

The effect of PG2212 on the expression of the major virulence factors in *P. gingivalis* is likely modulated via an indirect mechanism. Although gingipain activity was reduced in the PG_2212-deficient mutant, there was no observed alteration in the expression of those genes. Thus, it is likely that the reduced gingipain activity could be linked to a PG2212-dependent posttranslational process. Posttranslational modification linked to glycosylation has been shown to be important to the maturation pathway of the gingipains (50). We have also previously shown that sialidase activity may be involved in gingipain activity and other virulence factors in *P. gingivalis* (51). In our study, the sialidase-encoding gene (PG_0352) was downregulated in *P. gingivalis* FLL366 (ΔPG_2212), which would be consistent with its role in gingipain biogenesis. Our data also suggest that other processes modulated by the ECF sigma factor could be involved. We previously reported that ECF sigma factor PG1660 can modulate gingipain activity by an unknown mechanism (9). PG_1660 was downregulated more than 3-fold in *P. gingivalis* FLL366 in comparison to the wild type.

Prokaryotic transcription factors can have dual activity as either activator or repressor (52–54). Activation or repression mediated by transcription factors is linked to the distance of the regulator-binding sites relative to promoters. The preferred sites for activators are located between nucleotide positions −80 and −30 (reviewed in references 55, 56, and 57). Repressor-binding sites are generally located downstream from nucleotide position −30 (reviewed in references 55 and 57). In the PG_2212-deficient mutant, several genes were both up- and downregulated. The promoter region of several of these genes contained conserved motifs close to the −80 region. In addition to being consistent with a common transcriptional regulator, it is also likely that it may act as an activator site. Under similar conditions, the ability of the rPG2212 to bind this region would support this hypothesis, although we cannot rule out the possibility that the expression profile of the PG_2212-deficient mutant involves multiple transcriptional regulators and is part of a complex regulatory network. Several transcriptional regulators, including ECF sigma factors, were upregulated in this mutant under conditions of oxidative stress. It is unclear what direct role PG2212 may play in their expression. Although we cannot rule out other experimental conditions that may facilitate binding of PG2212 to its own promoter sequence, expression of the PG_2212 gene does not appear to be autoregulated and could be involved in a housekeeping function(s) due to the ability of its promoter region to bind the sigma 70 factor. Thus, under normal anaerobic conditions PG2212 may regulate a subset of genes (e.g., PG_1167 and PG_1459). However, under conditions of oxidative stress, other genes that are involved in its protection are activated. Although PG_2212 is constitutively expressed, possibly through its transcriptional regulation by sigma 70, its upregulation in response to oxidative stress is influenced by a yet-to-be-identified regulator. Taken together, this study has provided further insights into oxidative stress and virulence regulation in *P. gingivalis*. The regulatory mechanism(s) of this protein needs to be further studied.

ACKNOWLEDGMENTS

This work was supported by Public Health Services grants DE13664, DE019730, DE019730 04S1, DE022508, and DE022724 from NIDCR (to H.M.F.).

REFERENCES

1. **Detert J, Pischon N, Burmester GR, Buttgereit F.** 2010. The association between rheumatoid arthritis and periodontal disease. Arthritis Res. Ther. **12:**218. http://dx.doi.org/10.1186/ar3106.
2. **Inaba H, Amano A.** 2010. Roles of oral bacteria in cardiovascular diseases—from molecular mechanisms to clinical cases: implication of periodontal diseases in development of systemic diseases. J. Pharmacol. Sci. **113:**103–109. http://dx.doi.org/10.1254/jphs.09R23FM.
3. **Henry LG, McKenzie RM, Robles A, Fletcher HM.** 2012. Oxidative stress resistance in *Porphyromonas gingivalis*. Future Microbiol. **7:**497–512. http://dx.doi.org/10.2217/fmb.12.17.
4. **Ueshima J, Shoji M, Ratnayake DB, Abe K, Yoshida S, Yamamoto K, Nakayama K.** 2003. Purification, gene cloning, gene expression, and mutants of Dps from the obligate anaerobe *Porphyromonas gingivalis*. Infect. Immun. **71:**1170–1178. http://dx.doi.org/10.1128/IAI.71.3.1170-1178.2003.
5. **Sheets SM, Robles-Price AG, McKenzie RM, Casiano CA, Fletcher HM.** 2008. Gingipain-dependent interactions with the host are important for survival of *Porphyromonas gingivalis*. Front. Biosci. **13:**3215–3238. http://dx.doi.org/10.2741/2922.

6. **McKenzie RM, Johnson NN, Aruni W, Dou Y, Masinde G, Fletcher HM.** 2012. Differential response of *Porphyromonas gingivalis* to varying levels and duration of hydrogen peroxide-induced oxidative stress. Microbiology **158:**2465–2479. http://dx.doi.org/10.1099/mic.0.056416-0.
7. **Johnson NA, McKenzie R, McLean L, Sowers LC, Fletcher HM.** 2004. 8-Oxo-7,8-dihydroguanine is removed by a nucleotide excision repair-like mechanism in *Porphyromonas gingivalis* W83. J. Bacteriol. **186:**7697–7703. http://dx.doi.org/10.1128/JB.186.22.7697-7703.2004.
8. **Zheng M, Storz G.** 2000. Redox sensing by prokaryotic transcription factors. Biochem. Pharmacol. **59:**1–6. http://dx.doi.org/10.1016/S0006-2952(99)00289-0.
9. **Dou Y, Osbourne D, McKenzie R, Fletcher HM.** 2010. Involvement of extracytoplasmic function sigma factors in virulence regulation in *Porphyromonas gingivalis* W83. FEMS Microbiol. Lett. **312:**24–32. http://dx.doi.org/10.1111/j.1574-6968.2010.02093.x.
10. **Nelson KE, Fleischmann RD, DeBoy RT, Paulsen IT, Fouts DE, Eisen JA, Daugherty SC, Dodson RJ, Durkin AS, Gwinn M, Haft DH, Kolonay JF, Nelson WC, Mason T, Tallon L, Gray J, Granger D, Tettelin H, Dong H, Galvin JL, Duncan MJ, Dewhirst FE, Fraser CM.** 2003. Complete genome sequence of the oral pathogenic bacterium *Porphyromonas gingivalis* strain W83. J. Bacteriol. **185:**5591–5601. http://dx.doi.org/10.1128/JB.185.18.5591-5601.2003.
11. **Diaz PI, Slakeski N, Reynolds EC, Morona R, Rogers AH, Kolenbrander PE.** 2006. Role of *oxyR* in the oral anaerobe *Porphyromonas gingivalis*. J. Bacteriol. **188:**2454–2462. http://dx.doi.org/10.1128/JB.188.7.2454-2462.2006.
12. **Lewis JP, Iyer D, Anaya-Bergman C.** 2009. Adaptation of *Porphyromonas gingivalis* to microaerophilic conditions involves increased consumption of formate and reduced utilization of lactate. Microbiology **155:**3758–3774. http://dx.doi.org/10.1099/mic.0.027953-0.
13. **Duran-Pinedo AE, Nishikawa K, Duncan MJ.** 2007. The RprY response regulator of *Porphyromonas gingivalis*. Mol. Microbiol. **64:**1061–1074. http://dx.doi.org/10.1111/j.1365-2958.2007.05717.x.
14. **Tamura K, Dudley J, Nei M, Kumar S.** 2007. MEGA4: Molecular Evolutionary Genetics Analysis (MEGA) software version 4.0. Mol. Biol. Evol. **24:**1596–1599. http://dx.doi.org/10.1093/molbev/msm092.
15. **Johnson LS, Eddy SR, Portugaly E.** 2010. Hidden Markov model speed heuristic and iterative HMM search procedure. BMC Bioinformatics **11:**431. http://dx.doi.org/10.1186/1471-2105-11-431.
16. **Viklund H, Elofsson A.** 2004. Best alpha-helical transmembrane protein topology predictions are achieved using hidden Markov models and evolutionary information. Protein Sci. **13:**1908–1917. http://dx.doi.org/10.1110/ps.04625404.
17. **Eswar N, Webb B, Marti-Renom MA, Madhusudhan MS, Eramian D, Shen MY, Pieper U, Sali A.** 2007. Comparative protein structure modeling using MODELLER. Curr. Protoc. Protein Sci. **Chapter 2:**Unit 2.9. http://dx.doi.org/10.1002/0471140864.ps0209s50.
18. **Vriend G.** 1990. WHAT IF: a molecular modeling and drug design program. J. Mol. Graph. **8:**52–56, 29. http://dx.doi.org/10.1016/0263-7855(90)80070-V.
19. **Kanehisa M, Goto S, Furumichi M, Tanabe M, Hirakawa M.** 2010. KEGG for representation and analysis of molecular networks involving diseases and drugs. Nucleic Acids Res. **38:**D355–D360. http://dx.doi.org/10.1093/nar/gkp896.
20. **Hou BK, Kim JS, Jun JH, Lee DY, Kim YW, Chae S, Roh M, In YH, Lee SY.** 2004. BioSilico: an integrated metabolic database system. Bioinformatics **20:**3270–3272. http://dx.doi.org/10.1093/bioinformatics/bth363.
21. **Chang A, Scheer M, Grote A, Schomburg I, Schomburg D.** 2009. BRENDA, AMENDA and FRENDA the enzyme information system: new content and tools in 2009. Nucleic Acids Res. **37:**D588–D592. http://dx.doi.org/10.1093/nar/gkn820.
22. **Bairoch A.** 2000. The ENZYME database in 2000. Nucleic Acids Res. **28:**304–305. http://dx.doi.org/10.1093/nar/28.1.304.
23. **Henry LG, Sandberg L, Zhang K, Fletcher HM.** 2008. DNA repair of 8-oxo-7,8-dihydroguanine lesions in *Porphyromonas gingivalis*. J. Bacteriol. **190:**7985–7993. http://dx.doi.org/10.1128/JB.00919-08.
24. **Fletcher HM, Schenkein HA, Morgan RM, Bailey KA, Berry CR, Macrina FL.** 1995. Virulence of a *Porphyromonas gingivalis* W83 mutant defective in the *prtH* gene. Infect. Immun. **63:**1521–1528.
25. **Abaibou H, Chen Z, Olango GJ, Liu Y, Edwards J, Fletcher HM.** 2001. *vimA* gene downstream of *recA* is involved in virulence modulation in *Porphyromonas gingivalis* W83. Infect. Immun. **69:**325–335. http://dx.doi.org/10.1128/IAI.69.1.325-335.2001.
26. **Gardner RG, Russell JB, Wilson DB, Wang GR, Shoemaker NB.** 1996. Use of a modified *Bacteroides-Prevotella* shuttle vector to transfer a reconstructed beta-1,4-D-endoglucanase gene into Bacteroides uniformis and *Prevotella ruminicola* B(1)4. Appl. Environ. Microbiol. **62:**196–202.
27. **Vanterpool E, Roy F, Sandberg L, Fletcher HM.** 2005. Altered gingipain maturation in *vimA*- and *vimE*-defective isogenic mutants of *Porphyromonas gingivalis*. Infect. Immun. **73:**1357–1366. http://dx.doi.org/10.1128/IAI.73.3.1357-1366.2005.
28. **Palmer I, Wingfield PT.** 2012. Preparation and extraction of insoluble (inclusion-body) proteins from *Escherichia coli*. Curr. Protoc. Protein Sci. **Chapter 6:**Unit6.3. http://dx.doi.org/10.1002/0471140864.ps0603s70.
29. **Steinle A, Li P, Morris DL, Groh V, Lanier LL, Strong RK, Spies T.** 2001. Interactions of human NKG2D with its ligands MICA, MICB, and homologs of the mouse RAE-1 protein family. Immunogenetics **53:**279–287. http://dx.doi.org/10.1007/s002510100325.
30. **Vanterpool E, Roy F, Fletcher HM.** 2004. The *vimE* gene downstream of *vimA* is independently expressed and is involved in modulating proteolytic activity in *Porphyromonas gingivalis* W83. Infect. Immun. **72:**5555–5564. http://dx.doi.org/10.1128/IAI.72.10.5555-5564.2004.
31. **Lamont RJ, Jenkinson HF.** 1998. Life below the gum line: pathogenic mechanisms of *Porphyromonas gingivalis*. Microbiol. Mol. Biol. Rev. **62:**1244–1263.
32. **Antelmann H, Helmann JD.** 2011. Thiol-based redox switches and gene regulation. Antioxid. Redox Signal. **14:**1049–1063. http://dx.doi.org/10.1089/ars.2010.3400.
33. **Choi H, Kim S, Mukhopadhyay P, Cho S, Woo J, Storz G, Ryu SE.** 2001. Structural basis of the redox switch in the OxyR transcription factor. Cell **105:**103–113. http://dx.doi.org/10.1016/S0092-8674(01)00300-2.
34. **Dubbs JM, Mongkolsuk S.** 2012. Peroxide-sensing transcriptional regulators in bacteria. J. Bacteriol. **194:**5495–5503. http://dx.doi.org/10.1128/JB.00304-12.
35. **Ortiz de Orue Lucana D, Wedderhoff I, Groves MR.** 2012. ROS-mediated signalling in bacteria: zinc-containing Cys-X-X-Cys redox centres and iron-based oxidative stress. J. Signal Transduct. **2012:**605905. http://dx.doi.org/10.1155/2012/605905.
36. **Klug A.** 2010. The discovery of zinc fingers and their applications in gene regulation and genome manipulation. Annu. Rev. Biochem. **79:**213–231. http://dx.doi.org/10.1146/annurev-biochem-010909-095056.
37. **Krishna SS, Majumdar I, Grishin NV.** 2003. Structural classification of zinc fingers: survey and summary. Nucleic Acids Res. **31:**532–550. http://dx.doi.org/10.1093/nar/gkg161.
38. **Hoffman RC, Horvath SJ, Klevit RE.** 1993. Structures of DNA-binding mutant zinc finger domains: implications for DNA binding. Protein Sci. **2:**951–965. http://dx.doi.org/10.1002/pro.5560020609.
39. **Chou AY, Archdeacon J, Kado CI.** 1998. *Agrobacterium* transcriptional regulator Ros is a prokaryotic zinc finger protein that regulates the plant oncogene *ipt*. Proc. Natl. Acad. Sci. U. S. A. **95:**5293–5298. http://dx.doi.org/10.1073/pnas.95.9.5293.
40. **McAlister V, Zou C, Winslow RH, Christie GE.** 2003. Purification and in vitro characterization of the *Serratia marcescens* NucC protein, a zinc-binding transcription factor homologous to P2 Ogr. J. Bacteriol. **185:**1808–1816. http://dx.doi.org/10.1128/JB.185.6.1808-1816.2003.
41. **Lee TC, Christie GE.** 1990. Purification and properties of the bacteriophage P2 *ogr* gene product. A prokaryotic zinc-binding transcriptional activator. J. Biol. Chem. **265:**7472–7477.
42. **Janczarek M, Skorupska A.** 2007. The *Rhizobium leguminosarum* bv. trifolii RosR: transcriptional regulator involved in exopolysaccharide production. Mol. Plant Microbe Interact. **20:**867–881. http://dx.doi.org/10.1094/MPMI-20-7-0867.
43. **Rinaudi LV, Sorroche F, Zorreguieta A, Giordano W.** 2010. Analysis of the *mucR* gene regulating biosynthesis of exopolysaccharides: implications for biofilm formation in *Sinorhizobium meliloti* Rm1021. FEMS Microbiol. Lett. **302:**15–21. http://dx.doi.org/10.1111/j.1574-6968.2009.01826.x.
44. **Bittinger MA, Handelsman J.** 2000. Identification of genes in the RosR regulon of *Rhizobium etli*. J. Bacteriol. **182:**1706–1713. http://dx.doi.org/10.1128/JB.182.6.1706-1713.2000.
45. **Hussain H, Johnston AW.** 1997. Iron-dependent transcription of the regulatory gene *ros* of *Agrobacterium radiobacter*. Mol. Plant Microbe Interact. **10:**1087–1093. http://dx.doi.org/10.1094/MPMI.1997.10.9.1087.
46. **Lee KC, Yeo WS, Roe JH.** 2008. Oxidant-responsive induction of the suf operon, encoding a Fe-S assembly system, through Fur and IscR in *Escherichia coli*. J. Bacteriol. **190:**8244–8247. http://dx.doi.org/10.1128/JB.01161-08.

47. **Yeo WS, Lee JH, Lee KC, Roe JH.** 2006. IscR acts as an activator in response to oxidative stress for the suf operon encoding Fe-S assembly proteins. Mol. Microbiol. **61:**206–218. http://dx.doi.org/10.1111/j.1365-2958.2006.05220.x.
48. **Giel JL, Rodionov D, Liu M, Blattner FR, Kiley PJ.** 2006. IscR-dependent gene expression links iron-sulphur cluster assembly to the control of O2-regulated genes in *Escherichia coli*. Mol. Microbiol. **60:**1058–1075. http://dx.doi.org/10.1111/j.1365-2958.2006.05160.x.
49. **Schwartz CJ, Giel JL, Patschkowski T, Luther C, Ruzicka FJ, Beinert H, Kiley PJ.** 2001. IscR, an Fe-S cluster-containing transcription factor, represses expression of *Escherichia coli* genes encoding Fe-S cluster assembly proteins. Proc. Natl. Acad. Sci. U. S. A. **98:**14895–14900. http://dx.doi.org/10.1073/pnas.251550898.
50. **Muthiah AS, Aruni W, Robles AG, Dou Y, Roy F, Fletcher HM.** 2013. In *Porphyromonas gingivalis* VimF is involved in gingipain maturation through the transfer of galactose. PLoS One **8**(5):e63367. http://dx.doi.org/10.1371/journal.pone.0063367.
51. **Aruni W, Vanterpool E, Osbourne D, Roy F, Muthiah A, Dou Y, Fletcher HM.** 2011. Sialidase and sialoglycoproteases can modulate virulence in *Porphyromonas gingivalis*. Infect. Immun. **79:**2779–2791. http://dx.doi.org/10.1128/IAI.00106-11.
52. **Tapias A, Fernandez S, Alonso JC, Barbe J.** 2002. *Rhodobacter sphaeroides* LexA has dual activity: optimising and repressing *recA* gene transcription. Nucleic Acids Res. **30:**1539–1546. http://dx.doi.org/10.1093/nar/30.7.1539.
53. **Feng X, Oropeza R, Kenney LJ.** 2003. Dual regulation by phospho-OmpR of *ssrA/B* gene expression in *Salmonella* pathogenicity island 2. Mol. Microbiol. **48:**1131–1143. http://dx.doi.org/10.1046/j.1365-2958.2003.03502.x.
54. **Dutta R, Inouye M.** 1996. Reverse phosphotransfer from OmpR to EnvZ in a kinase-/phosphatase+ mutant of EnvZ (EnvZ.N347D), a bifunctional signal transducer of *Escherichia coli*. J. Biol. Chem. **271:**1424–1429. http://dx.doi.org/10.1074/jbc.271.3.1424.
55. **Gralla JD.** 1996. Activation and repression of *E. coli* promoters. Curr. Opin. Genet. Dev. **6:**526–530. http://dx.doi.org/10.1016/S0959-437X(96)80079-7.
56. **Tropel D, van der Meer JR.** 2004. Bacterial transcriptional regulators for degradation pathways of aromatic compounds. Microbiol. Mol. Biol. Rev. **68:**474–500. http://dx.doi.org/10.1128/MMBR.68.3.474-500.2004.
57. **Molina-Henares AJ, Krell T, Eugenia GM, Segura A, Ramos JL.** 2006. Members of the IclR family of bacterial transcriptional regulators function as activators and/or repressors. FEMS Microbiol. Rev. **30:**157–186. http://dx.doi.org/10.1111/j.1574-6976.2005.00008.x.